CHINESE OPTICS LETTERS

Vol. 21, No. 6 | June 2023

Wavelength-tunable dissipative soliton from Yb-doped fiber laser with nonlinear amplifying loop mirror

Yangyang Li (李杨阳), Man Jiang (江 曼)*, Lei Hou (侯 磊)**, Jianing Tao (陶家宁), Pengye Song (宋鹏棨), Baole Lu (陆宝乐), and Jintao Bai (白晋涛)

State Key Laboratory of Photon-Technology in Western China Energy, International Collaborative Center on Photoelectric Technology and Nano Functional Materials, Institute of Photonics & Photon Technology, School of Physics, Northwest University, Xi'an 710069, China

*Corresponding author: jmnwu@nwu.edu.cn

**Corresponding author: lhou@ustc.edu.cn

Received January 10, 2023 | Accepted April 4, 2023 | Posted Online June 6, 2023

We report a Yb-doped mode-locked fiber laser based on a nonlinear amplifying loop mirror (NALM), which is all-normal-dispersion (ANDi), and allows the output wavelength to be tunable. The laser can generate a stable femtosecond dissipative soliton with a maximum output power of 196 mW. Its repetition rate is 112.4 MHz, and the final pulse duration is 236 fs. By adjusting the angle of the reflective diffraction grating, the mode-locked fiber laser was realized to tune the output with a tuning range of 54 nm from 1011.8 nm to 1065.6 nm. To the best of our knowledge, this is the widest tuning range of an ANDi Yb-doped mode-locked fiber laser based on NALM.

Keywords: all-normal-dispersion; wavelength tuning; mode-locked fiber laser.

DOI: 10.3788/COL202321.061402

1. Introduction

The ultrafast fiber laser is one of the important development directions in laser technology. It has been widely used in scientific research and industries thanks to the superior characteristics of its compact structure, its ease of manufacture, and its high conversion efficiency[1–5]. Researchers have proposed soliton fiber lasers[6]. However, pulse energy for a single soliton is limited to about 0.1 nJ, due to the influence of soliton energy quantization[7]. To achieve a higher peak power to match the actual demand in different fields, it is usually necessary to manage the nonlinearity in fibers. In 2007, Chong *et al.* reported an all-normal-dispersion (ANDi) fiber laser that produced dissipative solitons[8]. Due to the interaction of dispersion and nonlinearity, and the balance of gain and loss, the dissipative solitons can maintain a single-pulse state at high peak power with a pulse energy output of about 20 nJ[9]. This type of laser increases the energy by many orders of magnitude compared to typical soliton lasers. Since then, the ANDi system has attracted much attention.

However, with the rapid development of spectroscopy, optical communication, sensing, medical, and industrial processing, the ultrafast laser with a single fixed wavelength cannot satisfy the increasing demands for multiple wavelengths light sources[10]. The ANDi fiber laser with a tunable output wavelength has become a hot topic of research. The broad fluorescence spectrum of Yb-doped fiber makes it more advantageous in a tunable ultrafast pulse source. In 2010, Kong *et al.* constructed an ANDi fiber laser using the principle of nonlinear polarization rotation (NPR), which realized 46.3 nm spectral tuning from 1024.5 nm to 1070.8 nm. However, increasing the pump power leads to a "blueshift" of the central wavelength of the dissipative soliton[11]. Since then, the ANDi systems using NPR to generate a multi-wavelength dissipative soliton have also been proposed. In the single-wavelength state, the wavelength tuning range of dissipative solitons is relatively narrow[12–15]. Because NPR is extremely sensitive to external disturbances, such as mechanical stress and temperature variation, the biggest problem of this type of laser is its poor stability[16]. On the other hand, due to the incompatibility between the polarization-maintaining (PM) fiber and NPR mechanism, it is difficult to solve these disturbances[17].

In 2014, Huang *et al.* reported a tunable and switchable multi-wavelength dissipative soliton generation in a graphene-oxide mode-locked Yb-doped fiber laser. In the single-wavelength mode-locked dissipative soliton state, continuous tuning can be achieved only by adjusting the polarization controller (PC), and the tuning wavelength range is 16.4 nm[18]. There are many real saturable absorbers used for the mode-locked device[19,20], but the deficiencies are obvious. First, the preparation of materials goes through a series of complex processes. It will greatly increase the experimental workload if commercial finished products are not used. Second, the ultrashort pulse power obtained with the material mode-locked device is always maintained at a low level, and once the threshold is exceeded, the

material will be damaged. It is worth noting that many saturable absorbers suffer from potential degradation over time, which is detrimental to the long-term operation of the laser. Therefore, the commercialization of a saturable absorber is limited[21,22]. Li *et al.* designed a figure-of-eight cavity ANDi fiber laser with a tuning range of 20 nm based on NALM[23]. Although its long-term stability is improved, the nonlinear effects will expand with a relatively long cavity[24]. Therefore, the search for an ANDi fiber laser with a high output power, a wide tuning range, and a long-term operational stability may provide a high-performance laser seed source for research in the field of optics.

In this paper, a tunable ANDi Yb-doped fiber laser with NALM is introduced. This NALM structure is without material degradation issues. At the same time, compared with the traditional figure-of-eight cavity, the cavity length is greatly shortened, and the structure is simplified. Using reflective grating as a filter and wavelength selective device, a stable dissipative soliton output is achieved, and the maximum output power of 196 mW can be obtained. The laser has a high repetition rate of 112.4 MHz and can generate femtosecond dissipative solitons. The pulse duration is 236 fs, which is achieved by a dechirped operation. Wavelength tuning was achieved through the rotation of reflective grating and variation of angle θ between the incident and reflected beams. We demonstrated a wavelength tuning range of 54 nm, and to the best of our knowledge, this value is the widest wavelength tuning range among those used in NALM as mode-locked devices.

2. Experimental Setup

The laser configuration is illustrated in Fig. 1. The pump light is a fiber-coupled 980 nm laser diode, which is input to the cavity by a 980/1060 nm wavelength division multiplexer (WDM). The total ring cavity length is only 1.25 m, including a 1.08 m fiber and a 0.17 m optical path in free space. In order to provide a sufficient differential nonlinear phase shift, a 0.21 m Yb-doped fiber (LIEKKI Yb1200-4/125) is asymmetrically placed in the nonlinear loop and acts as the gain medium of the laser. The group velocity dispersion (GVD) of the Yb-doped fiber is 24 ps^2/km. One end of the fiber optical coupler (2×2, 50/50) opens to form a linear arm in which the reflective diffraction grating (Thorlabs, GR13-0310), the polarization beam splitter (PBS), the phase shifter (FR and $\lambda/8$), and the collimator (Col) are placed in turn. The reflective grating has a linear density of 300 lines/mm, a blaze angle of 8°36′, and a reflection efficiency of 80% at 1030 nm, with the actual efficiency depending on the different polarization states[25]. The pigtails in the whole system are single-mode fibers (HI1060) with a GVD of 23 ps^2/km. Therefore, the total cavity net dispersion can be conveniently calculated to be approximately 0.029 ps^2.

When the pump power was set at 350 mW, a stable self-started mode-locked cavity can be realized. The phase shifter can provide an initial phase shift to the ring cavity, thereby improving the mode-locking capability of the cavity[26–28]. The output spectrum was monitored by an optical spectrum analyzer (OSA, Yokogawa, AQ6370C), the width of the pulse was measured by an autocorrelator (FR-103WS, Femtochrome Research Inc.), the pulse train was observed by a digital oscilloscope (MDO3054, Tektronix), and the signal-to-noise ratio (SNR) was obtained by a radio frequency (RF) spectrum analyzer (E4407B, Agilent Technologies Inc.).

3. Results and Discussion

A reflective diffraction grating was used as a filter and wavelength selector in the experiment. Figure 2 is the local amplification diagram of Fig. 1, which shows the principle of the grating tuning. The grating adopts the Littrow structure, that is, the strongest diffraction light will return to the cavity as feedback and form laser oscillation. At this time, the grating has the highest efficiency and also contributes to the high power output. For incident polychromatic light, different incident wavelengths λ have the same incident angle α, but the diffraction angles β are different. The normal direction of the grating is changed by rotating the reflective grating, which will cause the variation of the incident angle α, the center wavelength λ of the light entering the fiber collimator shifts, and the wavelength tuning is then realized.

Figure 3(a) depicts the relationship between the incident angle α and the center wavelength λ that can be received when the angle θ between the incident beam and the receiver is taken as a series of discrete constants (the spatial distance of the adjacent inscriptions $D = 1/300$ mm, diffraction order $m = 1$). It is shown that the reflective diffraction grating can realize the tuning of the wavelength in the range of 1 μm within the range of the receiving angle θ from 0° to 90°. Meanwhile, as indicated in Fig. 3(b), the distance between the grating and the collimator determines the filtering bandwidth. It can be proved that

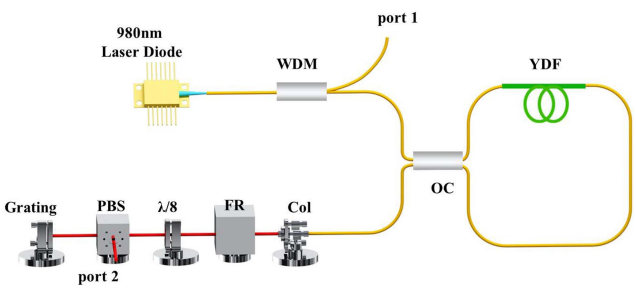

Fig. 1. Schematic setup of the mode-locked fiber laser with NALM.

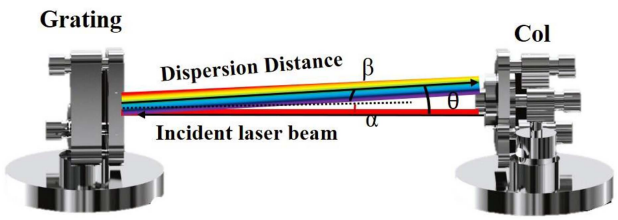

Fig. 2. Principle diagram of the reflective grating.

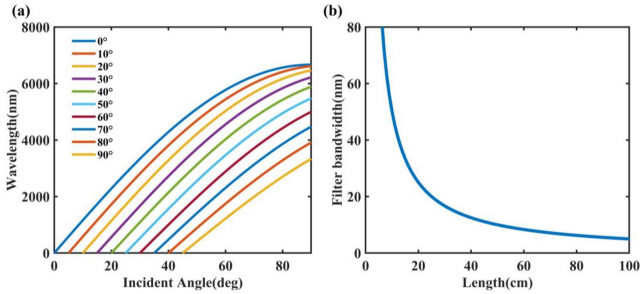

Fig. 3. (a) Relation between the incident angle α and the received center wavelength λ at different angle θ. (b) Variation in the filter bandwidth with the distance between the grating and the collimator.

there is a wide filtering bandwidth at a short distance, so the appropriate distance is fixed to ensure the feasibility of the experiment. We fix the distance to 0.17 m, which is the minimum distance for space devices to be placed.

The following figure illustrates the characteristics of the output pulses. All the results were measured at the pump power of 350 mW. In addition, the reflective grating was fixed at 9.5° to meet the output center wavelength of 1030.0 nm. The optical spectrum of ports 1 and 2 is shown in Figs. 4(a) and 4(c). The full-width at half-maximum (FWHM) is 11.8 nm and 7.32 nm; and the central wavelength is 1030.00 nm (spectrometer resolution: 0.02 nm). The autocorrelation trace of ports 1 and 2 is shown in Figs. 4(b) and 4(d). The corresponding autocorrelation trace with a sech^2 fitting is plotted with a pulse duration of 2.09 ps and 2.77 ps, respectively. Compared with port 1, the optical spectrum at port 2 is less smooth, which is induced by the intracavity interference of two backward propagation beams at port 2. Therefore, other characteristics of port 1 were observed and analyzed, and it provided much better pulse quality. The output spectrum of port 1 is a typical dissipative soliton with a cat-ear-like sideband and a time bandwidth product (TBP) of 6.97 for the soliton.

Figure 5(a) shows the variation of the average output power with the pump power. There is no continuous wave in the whole mode-locked range of the pump power from 220 mW to 970 mW, and the mode-locked fiber laser can remain constant. The maximum output power reaches 196 mW. The pulse train of the oscilloscope is presented in Fig. 5(b). The repetition rate of 112.4 MHz matches well with the total length of the cavity, and the pulse stability of the mode-locked fiber laser is confirmed by the pulse train with a time range of 1 μs. The radio frequency (RF) spectrum is shown in Fig. 5(c), with an SNR of 70 dB. The reason for the high SNR may be the suppression of noise by the equivalent saturable absorber and the effective excitation of gain by power[29]. Figure 5(d) shows the harmonics in the range of 80 MHz to 2000 MHz without modulation, indicating that the laser mode-locked in an excellent stable state.

Since the ANDi Yb-doped fiber laser has excellent output power, it is suitable for a dechirp operation to achieve femtosecond laser output. Therefore, we designed a grating pair compressor. The out-of-cavity compression scheme is illustrated in Fig. 6(a). The output laser from Col 1 enters the diffraction grating (LightSmyth Technologies, LSFSG-1000-3212-94, with linear density 1000 lines/mm) at an incident angle of 30° and a power of 68 mW, where the gratings are spaced by 32.5 mm and placed parallel to each other. After grating compression, the laser is reflected from HR 1 into Col 2 with a power of 43 mW and an overall compression efficiency of 63%. The autocorrelation trace of the dechirped pulse is given in Fig. 6(b), assuming the sech^2 pulse profile, the pulse duration of 236 fs, and the TBP of 1.1. However, the calculated Fourier transform limit pulse width is 94.467 fs, and the theoretical limit of the TBP is 0.315, which is different from the results obtained by us.

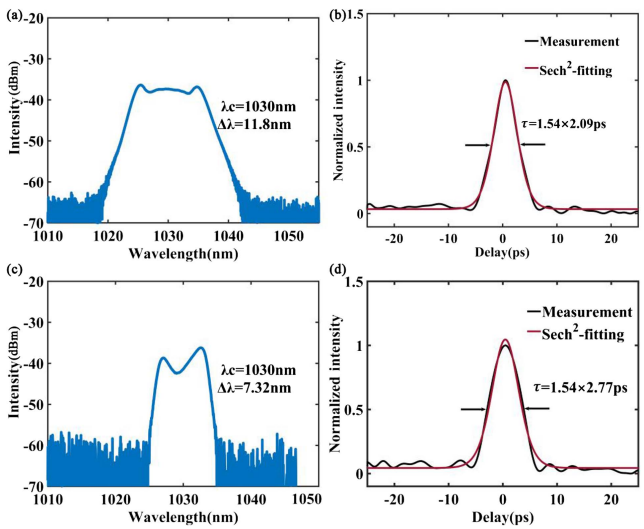

Fig. 4. Output characteristics of the fiber lasers. (a), (b) The output spectrum and the autocorrelation trace at port 1. (c), (d) The output spectrum and the autocorrelation trace at port 2.

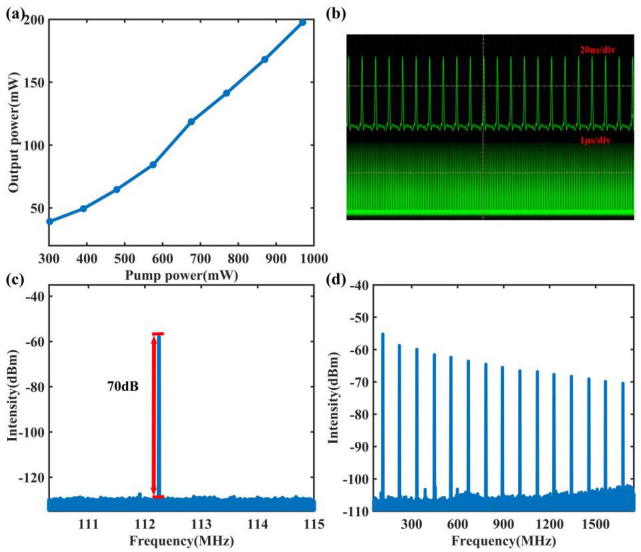

Fig. 5. (a) Output power versus pump power. (b) The oscilloscopic pulse train. (c) The RF spectrum of dissipative soliton, 5 MHz span with a 1 Hz resolution bandwidth. (d) The RF spectrum in 2 GHz with a resolution bandwidth of 200 Hz.

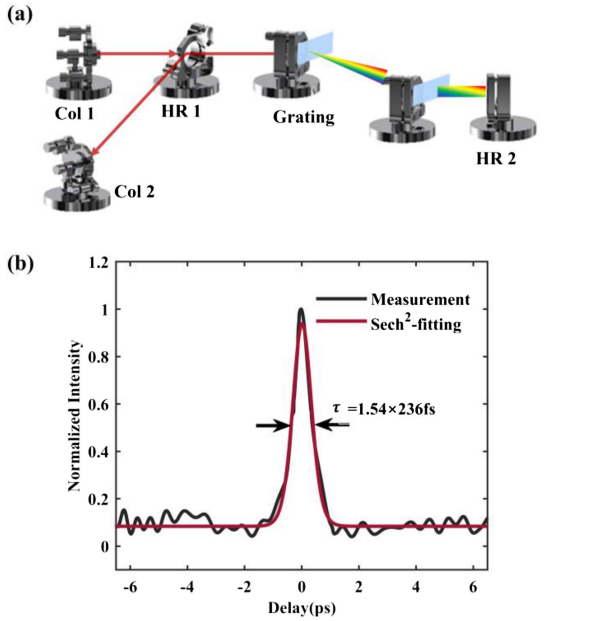

Fig. 6. (a) Schematic setup of the external cavity compression. (b) Corresponding autocorrelation trace.

The reasons are analyzed as follows. On the one hand, the grating pair compression scheme used in the experiment can only compensate for some of the linear chirps, while the nonlinear chirps are not compensated in the dissipative soliton pulse, which leads to the existence of chirps in the pulse so that it cannot approach the theoretical limit. On the other hand, the pulse width of the conventional soliton is usually close to the Fourier transform limit pulse width, which is due to the mutual compensation of the positive and negative chirps caused by the self-phase modulation and the dispersion effect during the formation of the conventional soliton in the anomalous dispersion region[30]. The chirp carried by the conventional soliton is very low, so the nonlinear phase shift that can be tolerated is extremely low. When the pulse energy is higher than the picojoule level, the conventional soliton is easy to split and produce harmonics or bound states. But for the dissipative solitons, the strong chirp is its characteristic. Therefore, dissipative solitons can withstand large phase shifts and can achieve single pulse output without splitting under high power conditions. Above all, the pulse width of the dissipative soliton pulse cannot be very close to the Fourier transform limit pulse width.

The tunability of the laser was investigated by rotating the reflective grating. In Fig. 7, the entire tunable wavelength range shows that the center wavelength was tuned from 1011.80 nm to 1065.64 nm, and the whole process is continuously tunable. The shape of the spectrum and the FWHM changed slightly during the process, which is caused by the large rotation angle that changes the nonlinear effects in the cavity[31]. No significant variation in pulse duration was observed for different central wavelengths. Meanwhile, arbitrary tuning directions are allowed. No matter whether it was going clockwise or anti-clockwise, for the rotation of the reflective grating angle (increasing θ and decreasing θ), there was no significant difference in the performance of the output pulse at the same wavelength.

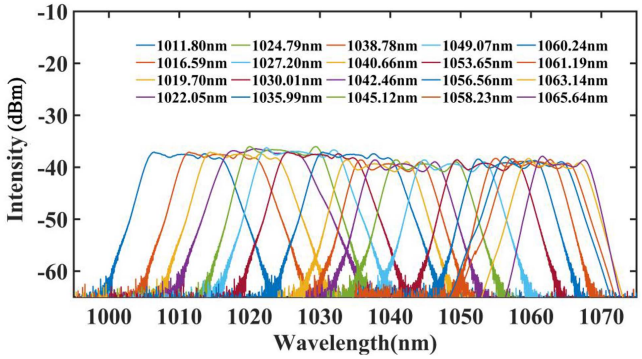

Fig. 7. Typical mode-locked spectral tuning range diagram (1011.80–1065.64 nm).

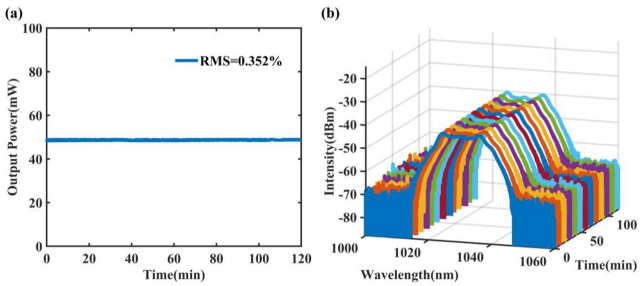

Fig. 8. (a) The power fluctuations of the laser output. (b) The spectra fluctuations of the laser output.

In order to further analyze the stability of the mode-locked laser, the relationship between the output power and the time was measured. As shown in Fig. 8(a), which displays the stability of the output power during 120 minutes, it can be seen that our laser has a good stability. The calculated root-mean-square (RMS) is approximately 0.352% at a pump power of 350 mW. On the other hand, the stability of the output spectrum was monitored. The laser spectrum at 1030 nm is depicted in Fig. 8(b), and there is no obvious shift of central wavelength or deformation during the two hours of observation, and a similar characteristic was observed over the entire tunable range.

4. Conclusion

In conclusion, we constructed the dissipative soliton Yb-doped mode-locked fiber laser. The laser operated in the ANDi regime, and a stable performance was obtained at a dechirped pulse duration of 236 fs, a repetition frequency of 112.4 MHz, and an SNR of 70 dB. Meanwhile, the wavelength tunability of the dissipative solitons was also investigated. Experimental results confirm that wavelength tuning is achieved in the range of 54 nm, covering 1011.80–1065.64 nm. The FWHM and shape of the output pulse spectrum do not change significantly throughout the tuning range. The output power and spectral

characteristics of the laser were monitored simultaneously, and excellent stability was proved. Compared with the traditional tunable ANDi Yb-doped fiber laser, the key advantages of our device are a high output power, a wide wavelength tuning range, and good stability. This laser will be an ideal choice as high-performance light source for tunable laser setups and high-power amplifiers.

Acknowledgement

This work was supported by the Natural Science Basic Research Plan in Shaanxi Province of China (No. 2021JM316), National Natural Science Foundation of China (No. 61905193), and International Cooperative Program (No. 2014DFR10780).

References

1. M. E. Fermann and I. Hartl, "Ultrafast fibre lasers," Nat. Photonics **7**, 868 (2013).
2. S. Lei, X. Zhao, X. Yu, A. Hu, S. Vukelic, M. B. G. Jun, H.-E. Joe, Y. L. Yao, and Y. C. Shin, "Ultrafast laser applications in manufacturing processes: a state-of-the-art review," J. Manuf. Sci. Eng. **142**, 031005 (2020).
3. U. Keller, "Recent developments in compact ultrafast lasers," Nature **424**, 831 (2003).
4. Y.-G. Han, T. V. A. Tran, S.-H. Kim, and S. B. Lee, "Multiwavelength Raman-fiber-laser-based long-distance remote sensor for simultaneous measurement of strain and temperature," Opt. Lett. **30**, 1282 (2005).
5. T. Kobayashi, "Development of ultrashort pulse lasers for ultrafast spectroscopy," Photonics **5**, 19 (2018).
6. V. Matsas, T. Newson, D. Richardson, and D. Payne, "Self-starting passively mode-locked fibre ring soliton laser exploiting nonlinear polarization rotation," Electron. Lett. **28**, 1391 (1992).
7. D. Tang, L. Zhao, B. Zhao, and A. Liu, "Mechanism of multisoliton formation and soliton energy quantization in passively mode-locked fiber lasers," Phys. Rev. A **72**, 043816 (2005).
8. A. Chong, W. H. Renninger, and F. W. Wise, "All-normal-dispersion femtosecond fiber laser with pulse energy above 20 nJ," Opt. Lett. **32**, 2408 (2007).
9. L. Hou, M. Li, X. He, Q. Lin, H. Guo, B. Lu, X. Qi, H. Chen, and J. Bai, "Wavelength-tunable dissipative pulses from Yb-doped fiber laser with Sagnac filter," Laser Phys. Lett. **13**, 125302 (2016).
10. J. Nilsson, W. A. Clarkson, R. Selvas, J. K. Sahu, P. W. Turner, S. U. Alam, and A. B. Grudinin, "High-power wavelength-tunable cladding-pumped rare-earth-doped silica fiber lasers," Opt. Fiber Technol. **10**, 5 (2004).
11. L. Kong, X. S. Xiao, and C. X. Yang, "Tunable all-normal-dispersion Yb-doped mode-locked fiber lasers," Laser Phys. **20**, 834 (2010).
12. Z. Zhang, Z. Xu, and L. Zhang, "Tunable and switchable dual-wavelength dissipative soliton generation in an all-normal-dispersion Yb-doped fiber laser with birefringence fiber filter," Opt. Express **20**, 26736 (2012).
13. H. Lin, C. Guo, S. Ruan, J. Yang, D. Ouyang, Y. Wu, and L. Wen, "Tunable and switchable dual-wavelength dissipative soliton operation of a weak-birefringence all-normal-dispersion Yb-doped fiber laser," IEEE Photon. J. **5**, 1501807 (2013).
14. S. Yang, X. Wang, M. Sun, and Q. Liang, "Wavelength switchable and tunable dissipative soliton Yb-doped fiber laser," Infrared Laser Eng. **49**, 128 (2020).
15. J. Cao, D. Sun, H. Zhuang, G. Zhang, L. Zou, Y. Ji, Y. Shi, Z. Han, and X. Zhu, "Multiple dissipative soliton Yb-doped fiber laser without an additional filter," Eur. Phys. J. D **75**, 1 (2021).
16. N. Kuse, J. Jiang, C.-C. Lee, T. R. Schibli, and M. E. Fermann, "All polarization-maintaining Er fiber-based optical frequency combs with nonlinear amplifying loop mirror," Opt. Express **24**, 3095 (2016).
17. W. Liu, R. Liao, J. Zhao, J. Cui, Y. Song, C. Wang, and M. Hu, "Femtosecond Mamyshev oscillator with 10-MW-level peak power," Optica **6**, 194 (2019).
18. S. Huang, Y. Wang, P. Yan, J. Zhao, H. Li, and R. Lin, "Tunable and switchable multi-wavelength dissipative soliton generation in a graphene oxide mode-locked Yb-doped fiber laser," Opt. Express **22**, 11417 (2014).
19. Q. Lin, L. Yan, Y. Song, X. Jia, X. Feng, L. Hou, and J. Bai, "Switchable single- and dual-wavelength femtosecond mode-locked Er-doped fiber laser based on carboxyl-functionalized graphene oxide saturable absorb," Chin. Opt. Lett. **19**, 111405 (2021).
20. C. Zhang, J. Liu, Y. Gao, X. Li, H. Lu, Y. Wang, J.-J. Feng, J. Lu, K. Ma, and X. Chen, "Porous nickel oxide micron polyhedral particles for high-performance ultrafast photonics," Opt. Laser Technol. **146**, 107546 (2022).
21. T. Hasan, Z. Sun, F. Wang, F. Bonaccorso, and P. Tan, "Nanotube–polymer composites for ultrafast photonics," Adv. Mater. **21**, 3874 (2009).
22. X. Zhao, Y. Liu, and L. Zhou, "All-normal-dispersion polarization-maintaining Yb-doped fiber laser based on nonlinear amplifying loop mirror," Chin. J. Lasers **46**, 0508025 (2019).
23. X. Li, Y. Wang, W. Zhao, W. Zhang, Z. Yang, X. H. Hu, H. S. Wang, X. Wang, Y. N. Zhang, Y. K. Gong, C. Li, and D. Y. Shen, "All-normal dispersion, figure-eight, tunable passively mode-locked fiber laser with an invisible and changeable intracavity bandpass filter," Laser Phys. **21**, 940 (2011).
24. J. Zhou and X. Gu, "32-nJ 615-fs stable dissipative soliton ring cavity fiber laser with Raman scattering," IEEE Photon. Technol. Lett. **28**, 453 (2016).
25. H. Guo, L. Hou, Y. Wang, J. Sun, Q. Lin, Y. Bai, and J. Bai, "Tunable ytterbium-doped mode-locked fiber laser based on single-walled carbon nanotubes," J. Lightwave Technol. **37**, 2370 (2019).
26. G. Liu, X. Jiang, A. Wang, G. Chang, F. Kaertner, and Z. Zhang, "Robust 700 MHz mode-locked Yb: fiber laser with a biased nonlinear amplifying loop mirror," Opt. Express **26**, 26003 (2018).
27. M. Li, W. Yang, Z. Zhang, and A. Wang, "Mode-locked femtosecond 910 nm Nd: fibre laser with phase biased non-linear loop mirror," Electron. Lett. **53**, 1479 (2017).
28. T. Jiang, Y. Cui, P. Lu, C. Li, A. Wang, and Z. Zhang, "All PM fiber laser mode locked with a compact phase biased amplifier loop mirror," IEEE Photon. Technol. Lett. **28**, 1786 (2016).
29. M. Yamada, "Analysis of intensity and frequency noises in semiconductor optical amplifier," J. Quantum Electron. **48**, 980 (2012).
30. X. Liu, "Interaction and motion of solitons in passively- mode-locked fiber lasers," Phys. Rev. A **84**, 053828 (2011).
31. X. Zhou, Y. J. Song, R. Liao, B. Liu, M. Hu, L. Chai, and Q. Wang, "Research on modified nonlinear amplifying loop mirror mode-locked lasers," Chin. J. Lasers **42**, 1202002 (2015).